

E. Observation and NWP in Southeast Asia

E-1. Towards a mesoscale observation network for Southeast Asia¹

Current conventional meteorological observations in Southeast Asia are clustered around the coastal regions due to the maritime nature and unique topography of the region. Coupled with the standard time interval of 6 to 12 hours between sampling, the region's conventional observation network lacks the spatial and temporal resolution to adequately capture the convective weather systems dominant in the region for weather forecasting and research.

The deployment of a transnational mesoscale testbed comprising ground-based remote and in situ sensors around the Straits of Malacca to investigate the Sumatra squalls could be a possible first step towards realizing a Southeast Asian mesoscale observation network. Improvement to the regional observational network could be achieved in parallel through integrating the existing weather radars operated by the various national weather agencies. Promoting the judicious use of weather satellite data in weather forecast and research should augment the lack of weather observations over the seas. These radar and satellite data if optimally assimilated, is expected to improve NWP forecast accuracies given the current dearth of conventional observations.

Although the sharing of radar data and the assimilation of more satellite data would be significant initial steps forward, more could be achieved through gradual, sustained and coordinated regional efforts in deploying in situ and remote-sensing instruments first in testbeds, but eventually as multi-sensor weather monitoring clusters. The mature mesoscale observation network is envisioned to comprise several coordinated radar, remote sensor subnets, in situ instruments, and satellite data receiving stations (Koh and Teo 2009). Due to the region's rich diversity, managing this mesoscale observation network could be through a confederation of the national or private stakeholders of this network (Fig. E-1-1). Apart from benefiting weather forecasts, the data collected by the network would act as a stimulus for much needed research into Southeast Asian weather systems.

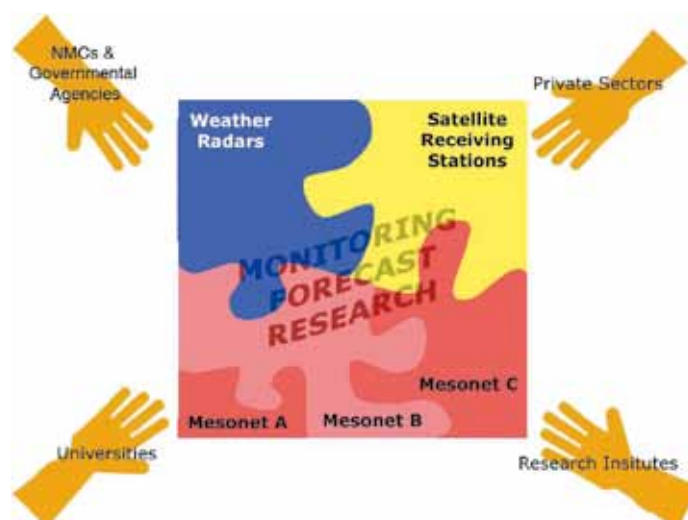


Fig. E-1-1. Schematic diagram of the envisioned mesoscale observation network with its component subnets and various stakeholders. After Koh and Teo (2009).

¹ T.-Y. Koh and C.-K. Teo (NTU)

E-2. Development of Operational Rapid Update Non-hydrostatic NWP Model and Data Assimilation System in the Hong Kong Observatory¹

E-2-1. Introduction of NWP System in HKO

A mesoscale NWP model system has been operated by the Hong Kong Observatory (HKO) using the Operational Regional Spectral Model (ORSM) since 1999. ORSM is formulated using the hydrostatic governing equations to provide numerical model guidance for short-term weather prediction up to 3 days ahead. The finest horizontal resolution is 20 km and the model run is updated every 3 hours. With the recent advances made in NWP modeling, HKO commenced the implementation and experimental trials of non-hydrostatic models a few years ago, with a view to enhance the capability of quantitative precipitation forecast (QPF) and prediction of severe weather phenomena and mesoscale convective systems. In April 2004, HKO started to operate the JMA Non-hydrostatic Model (NHM) (Saito *et al.* 2006) in trial basis to provide very-short-range (1-12 hours) forecasts which are rapidly updated at every hour with a high resolution (grid spacing at 5 km) covering an area of about 600 km x 600 km centred over Hong Kong. The initial and boundary conditions are obtained from the ORSM. In order to reduce the spin-up time of the model and improve the model QPF, the specific humidity fields of the cloud hydrometeors in NHM are initialized by the 3-dimensional cloud analysis output from the Local Analysis and Prediction System (LAPS) (Albers *et al.* 1996). Radar reflectivity, Doppler radial wind and geostationary satellite cloud data (visible albedo and infrared brightness temperature) are ingested into LAPS to generate the humidity fields of hydrometeors. Improvements in model QPF are obtained that facilitate the development of blending technique with nowcast QPF (Wong and Lai 2006). At the same time, forecasts from NHM are used to provide background data to LAPS for mesoscale real-time analysis with horizontal resolutions from few kilometres to few hundreds metres.

With experience gained on using JMA-NHM over the last few years, HKO has developed a new NWP system based on NHM, also called the Atmospheric Integrated Rapid cycle (AIR) forecast model system, and has been put into operation since June 2010. AIR forecast model system has two forecast domains with horizontal resolutions at 10 km and 2 km. With substantial increase in the horizontal resolution, use of non-hydrostatic governing equations and more advance model physics, the new system enhances the capability to resolve mesoscale and local-scale weather phenomena, and their evolution from very-short-range to 3 days ahead.

In this paper, the design and experimental results of the AIR forecast model system are described. In the next two sections, specifications of NHM and its data assimilation system will be presented. Performance of NHM in a couple of case studies on QPF, tropical cyclone movement and intensity, as well as the model verification on upper-level wind forecasts against aircraft data will be illustrated in E-2-4. A short summary including aspects of future research and development of AIR system will be given in section E-2-5.

¹ W.K. Wong

E-2-2. Description of NHM in AIR Forecast Model System

Figure E-2-1 shows the coverage of the two NHM domains in AIR forecast model system. The outer domain, denoted by Meso-NHM, has the horizontal resolution of 10 km with 50 terrain-following vertical levels. Meso-NHM has an analysis-forecast cycle of 3 hours to provide the forecast up to 72 hours ahead. It is targeted to simulate rainstorm, tropical cyclone track and intensity, and other mesoscale weather systems. The boundary condition of Meso-NHM is obtained from the forecasts of JMA Global Spectral Model (GSM; JMA 2007) that are updated every 6 hours (initial times at 00, 06, 12 and 18 UTC) with a horizontal resolution of forecast data at 0.5 degree in latitude and longitude. The sea-surface temperature (SST) is specified by the NCEP high resolution real-time daily SST analysis at 0.083 degree. The inner domain, called the RAPIDS-NHM, has a horizontal resolution of 2 km with 60 vertical levels. Its boundary condition is based on the forecasts from Meso-NHM. RAPIDS-NHM provides forecasts up to 15 hours ahead and the model forecast is rapidly updated at every hour with a view to enhance the analysis and prediction of mesoscale and convective weather phenomena as well as to provide an improved model QPF to blend with the radar-based precipitation nowcast. More details on the specification of Meso-NHM and RAPIDS-NHM are given in Table E-2-1.

E-2-3. Data Assimilation System of AIR/NHM

The data assimilation of NHM in AIR forecast model system is developed on the basis of JNoVA-3DVAR (JMA Non-hydrostatic model based Variational data Assimilation system). It is implemented as the hourly analysis system in JMA and the design is originated from the JNoVA-4DVAR (Honda *et al.* 2005) which is the operational data assimilation system for JMA Mesoscale Model (MSM) using NHM with a horizontal resolution of 5 km (JMA 2007). Like the other variational data assimilation system, JNoVA-3DVAR computes the best linear unbiased estimate of the control variables representing the model states that minimize the following cost function:

$$J(\mathbf{x}) = \frac{1}{2}(\mathbf{x} - \mathbf{x}_B)\mathbf{B}(\mathbf{x} - \mathbf{x}_B)^T + \frac{1}{2}(\mathbf{y} - \mathbf{H}\mathbf{x})\mathbf{R}(\mathbf{y} - \mathbf{H}\mathbf{x})^T ,$$

where \mathbf{x} , \mathbf{x}_B are respectively control variable vector and model background field. They include horizontal wind components (u, v), surface pressure (p_s), potential temperature (θ) and pseudo relative humidity representing the ratio of specific humidity of water vapour to its saturation value. \mathbf{y} represents a state vector containing observation data and \mathbf{H} is the observation operator. \mathbf{B} and \mathbf{R} are respectively observation and background error covariance matrices where \mathbf{B} matrix is estimated based on the NMC method (Parrish and Derber 1992).

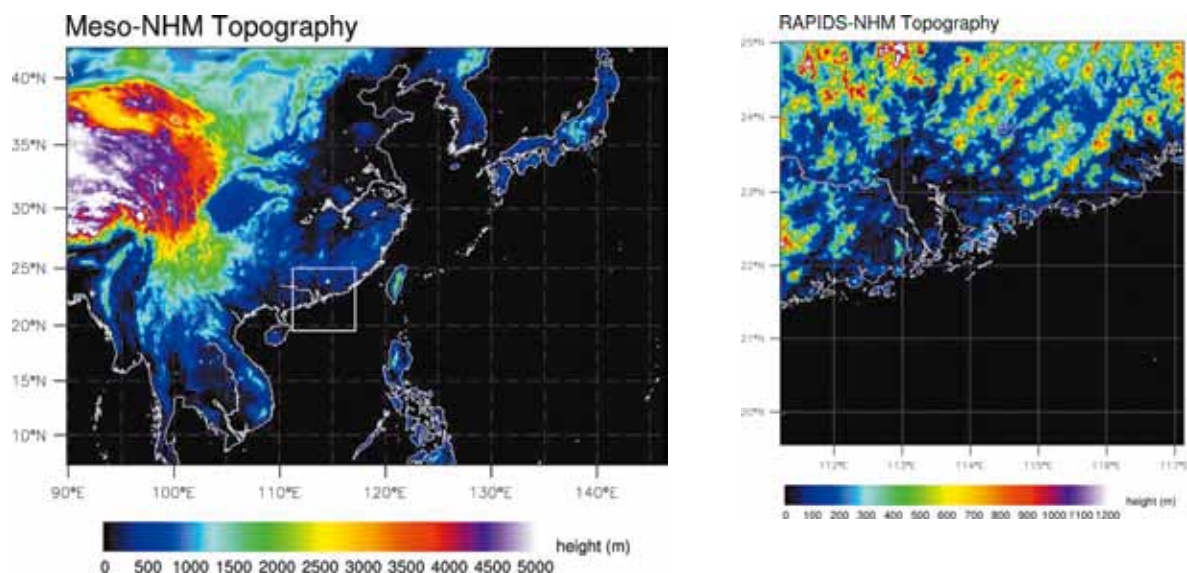


Fig. E-2-1. Spatial coverage of Meso-NHM and RAPIDS-NHM. Altitude of model topography (in metre) is given in color shading.

Table. E-2-1. Specification of Meso-NHM and RAPIDS-NHM in AIR Forecast Model System.

	Meso-NHM	RAPIDS-NHM
Horizontal resolution	10 km	2 km
Horizontal grid	Arakawa-C	
Map projection	Mercator	
No. of grid points	585x405	305x305
Vertical coordinates	Terrain following height coordinates using Lorenz grid	
No. of vertical levels	50	60
Time step	30 s	8 s
Initial time	00, 03, 06,..., 21 UTC	Every hour
Forecast range	72 hours	15 hours
Initial condition	JNoVA-3DVAR with background from JMA GSM forecast	JNoVA-3DVAR with background from Meso-NHM
Boundary condition	JMA GSM forecast data at 0.5 degree resolution in lat/lon	Meso-NHM forecasts
Nesting configuration	One-way nesting	
Topography	USGS GTOPO30 (30 second data smoothed to 1.5 times horizontal resolution) with modifications over HK areas based on USGS-SRTM (Shuttle Radar Topography Mission)	
Land-use characteristics	USGS Global Land Cover Characterization (GLCC) 30 second data and 24 land-use types with modification over HK areas	
Dynamics	Fully compressible non-hydrostatic governing equations solved by time-splitting horizontal-explicit-vertical-implicit (HEVI) scheme using 4-order centred finite differencing in flux form	
Cloud microphysics	3-ice bulk microphysics scheme	
Convective parameterization	Kain-Fritsch scheme (JMA version)	-
Surface process	Flux and bulk coefficients: Beljaars and Holtslag (1991), Donelan et al. (2004), Belamari (2005); Roughness length: Beljaars (1995) and Fairall et al. (2003); Stomatal resistance and temporal change of wetness included; 4-layer soil model to predict ground temperature and surface heat flux.	
Turbulence closure model and planetary boundary layer process	Mellor-Yamada-Nakanishi-Niino Level 3 (MYNN-3) (Nakanishi and Niino, 2004) with partial condensation scheme (PCS) and implicit vertical turbulent solver. Height of PBL calculated from virtual potential temperature profile.	
Atmospheric radiation	Long wave radiation process follows Kitagawa (2000) Short wave radiation process using Yabu and Kitagawa (2005) Prognostic surface temperature included; Cloud fraction determined from PCS.	

The observation data that can be assimilated in JNoVA-3DVAR include conventional observations from synoptic weather stations, radiosonde, buoy and ship reports, as well as data from automatic weather stations in Hong Kong and the Guangdong province, wind profilers, aircraft (AMDAR reports), atmospheric motion vector (AMV) from MTSAT-1R/MTSAT-2 geostationary satellite and retrieved ATOVS (Advanced TIROS Operational Vertical Sounder) temperature profile from NOAA polar-orbiting satellites. Total precipitable water vapour (TPWV) retrieved from microwave sounders (SSM/I and AMSR-E) is ingested in the Meso-NHM analysis, while TPWV from the local Global Positioning System (GPS) network signals are assimilated in RAPIDS-NHM to analyse the humidity contents. For the initialization of tropical cyclone, JNoVA-3DVAR includes a bogus scheme that is based on the forecaster's analysis on central pressure, maximum wind and radius of strong wind to construct vertical profiles of horizontal wind components around the tropical cyclones, with asymmetric effects of storm structure taken into account. The wind profiles are then assimilated into JNoVA-3DVAR in a similar way as the other upper-air wind data but using different error characteristics. Furthermore, Doppler radial velocity data from the two weather radars in Hong Kong are also assimilated in RAPIDS-NHM analysis.

E-2-4. Case Studies

In this section, discussions will be given to illustrate the performance of NHM in a couple of cases on significant convection and tropical cyclone forecasts. Verification on the analysis and forecast performance of NHM on weather elements and a comparison with ORSM will also be discussed.

a. Rainstorm on 24 May 2009

On 24 May 2009, a broad area of low pressure affected the northern part of the South China Sea. Meanwhile, a ridge of high pressure was established over southeastern part of China that resulted in convergence of easterly and southerly airstreams and successive development of rainbands over the coastal areas (Fig. E-2-2a - c). Figure E-2-3a depicts the forecasts of sea-level pressure and hourly accumulated rainfall at 0400 UTC on 24 May 2009 from Meso-NHM initialized at 1800 UTC on 23 May. Meso-NHM can successfully simulate the rainbands over the coastal water. It can be revealed from the forecasts of winds and relative humidity on 850 hPa and 700 hPa levels (Figs. E-2-3b and E-2-3c) that the development of the rainbands was associated with the low-level jet of moist southeasterly winds (areas enclosed by the red isotach representing 20 knots and above). As the convection predicted by Meso-NHM is quite shallow, the precipitation forecast by the model is less than the actual rainfall from radar estimate. Figure E-2-3d shows the forecast at the same time by RAPIDS-NHM which is initialized by the 3-hour forecast from Meso-NHM including the mixing ratio of the cloud hydrometeors. In general, the forecasted rainbands from RAPIDS-NHM have more detailed structures due to increased horizontal resolution, which are more consistent with the rainbands shown on the radar imagery in terms of their size and orientation in northwest-southeast direction.

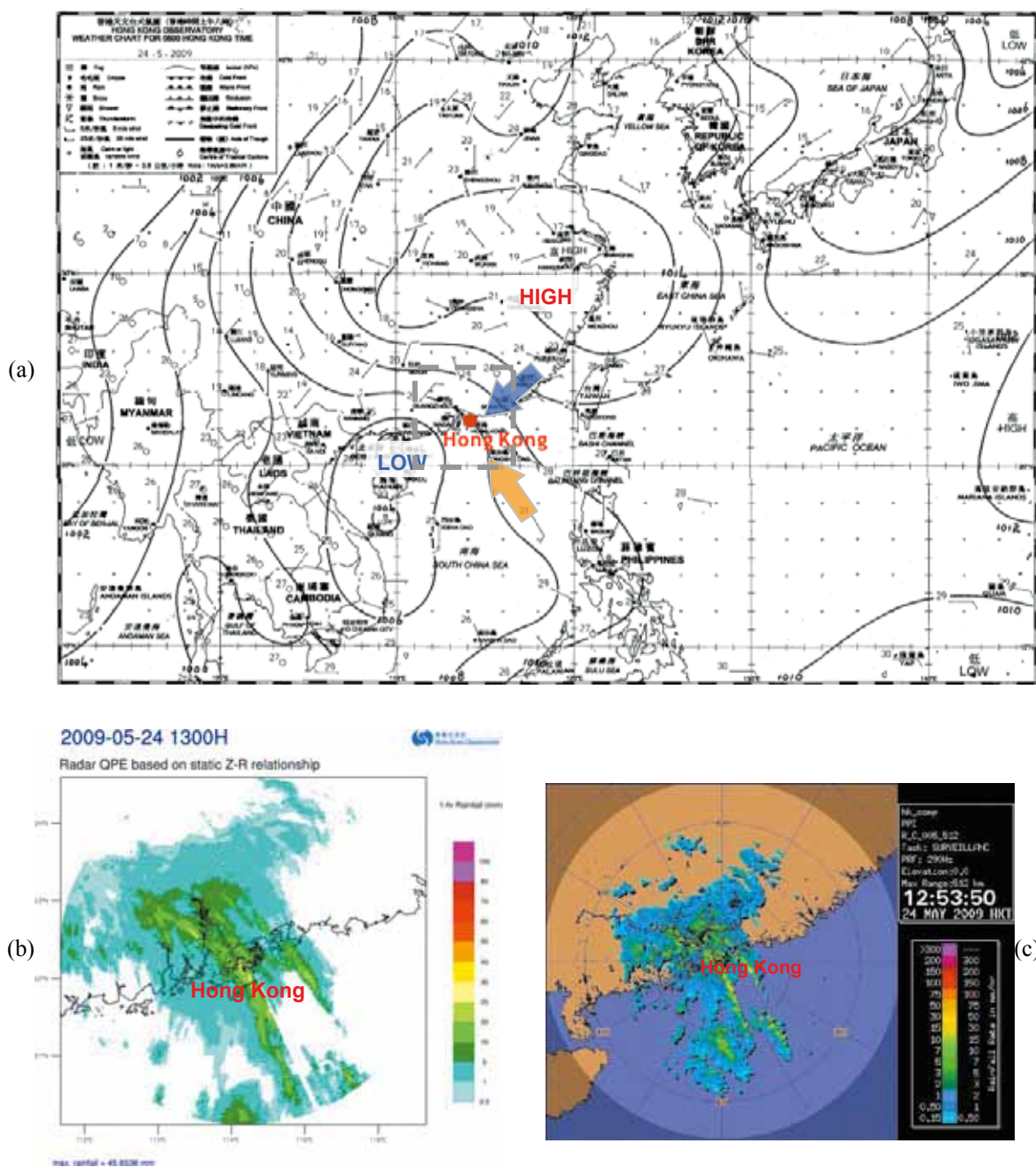


Fig. E-2-2. (a) Synoptic analysis at 0000 UTC (0800 HKT) 24 May 2009 (0800 HKT); (b) Radar rainfall analysis of 1-hr accumulated rainfall (in mm) at 1300 HKT and its spatial coverage is shown by grey dash line in (a); (c) radar reflectivity imagery at 1253 HKT.

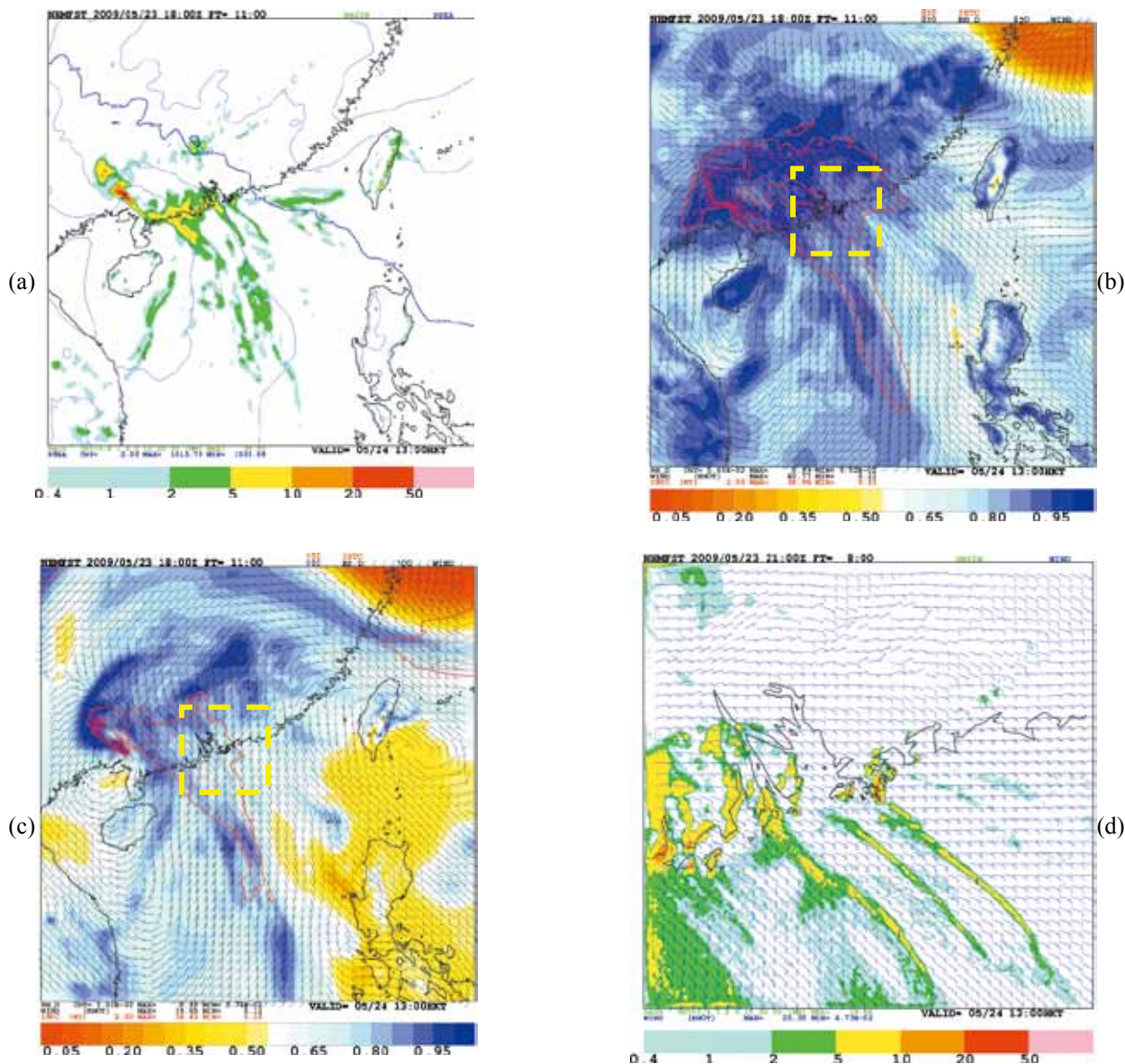


Fig. E-2-3. (a) Forecast of sea-level pressure and 1-hour accumulated rainfall (in mm) at 1200 HKT 24 May 2009 by Meso-NHM; Forecast of relative humidity (color in percentage) and winds on (b) 850 hPa and (c) 700 hPa levels, areas enclosed by red contour representing wind speed exceeding 20 knots; (d) Forecast of 1-hour accumulated rainfall and surface wind at 1200 HKT by RAPIDS-NHM. Coverage of RAPIDS-NHM is shown in yellow dash line in (b) and (c).

b. Typhoon Koppu (0915) – Effects of bogus in TC intensity analysis and forecast

Figure E-2-4a shows the 3DVAR analysis of Meso-NHM on the surface wind and sea-level pressure of tropical cyclone Koppu (0915) at 1200 UTC 13 September 2009. Bogus wind profiles are assimilated in the analysis. At that time, Koppu had just intensified into a tropical storm with maximum wind at about 35 knots. The analysed central pressure is 991 hPa that agrees with the forecaster’s real-time analysis. Compared to the background field (Fig. E-2-4d) as interpolated by the GSM forecasts, the intensity of Koppu is improved through the bogus data assimilation as the central pressure is deepened by about 10 hPa. The 24 hour and 48 hour of forecasts using the above 3DVAR analysis (first guess from GSM) as initial conditions are given in Figs. E-2-4b and c (E-2-4e and f),

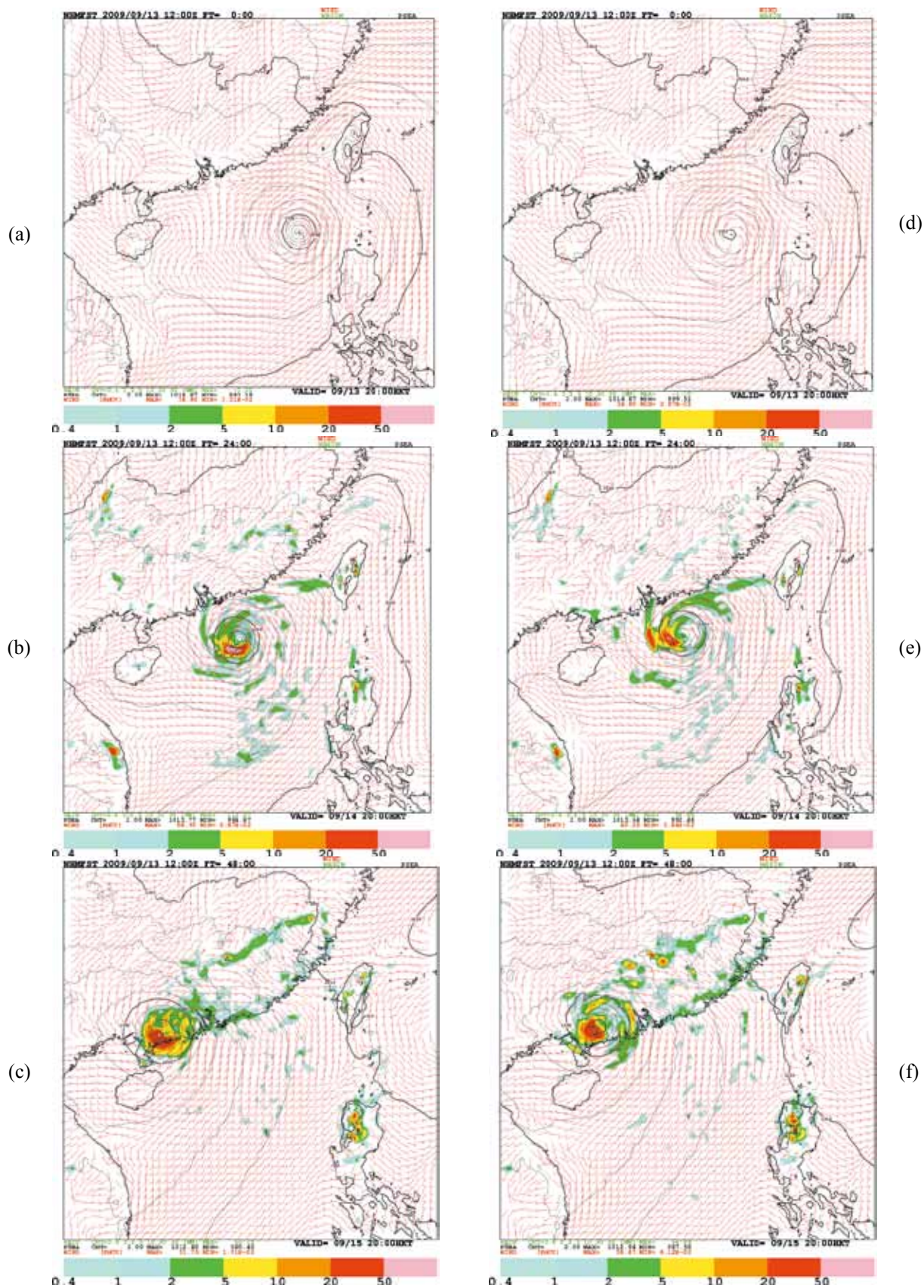


Fig. E-2-4. (a) JNoVA-3DVAR analysis of surface wind, sea-level pressure at 12 UTC 13 September 2009 by Meso-NHM; (b)-(c) 24 hour and 48 hours forecast overlaid with 1-hour accumulated rainfall (color in mm). Corresponding initial field and forecasts without 3DVAR analysis are shown in (d)-(f).

respectively. The forecast tracks are shown in Fig. E-2-5a, indicating that tracks from the two experiments are quite similar, although the time of landfall from the two experiments both lag behind the actual track by about 12 hours. Nevertheless, the bogus data assimilation results in a better intensification trend of Koppu (Fig. E-2-5b) as the winds on upper levels within the bogus region are strengthened. The maximum wind speed (MWS) near surface is increased by 22 knots in the 24 hour forecasts with bogus data assimilation while MWS is increased by only 5 knots in the other case.

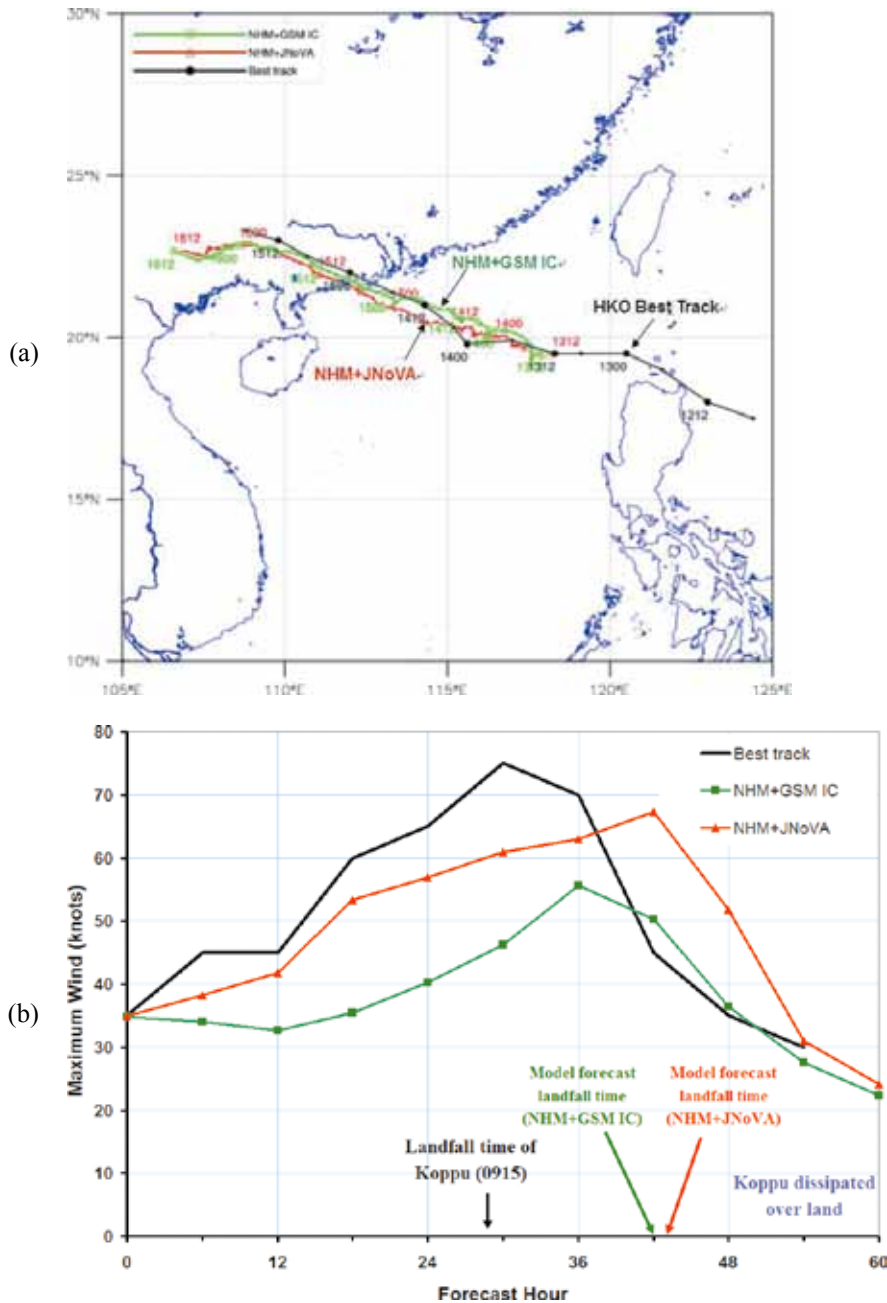


Fig. E-2-5. (a) Forecast tracks of Koppu (0915) by Meso-NHM using JNoVA-3DVAR analysis (red line with triangle marks) and initial condition interpolated from GSM forecast (green line with square marks). HKO best track is shown in black line with dots indicating the 6-hourly positions; (b) Maximum wind near centre of Koppu by the two experiments. HKO best track data is shown in black line.

c. *Severe thunderstorm on 8 September 2010*

In late evening on 8 September 2010 to the following early morning, widespread thunderstorms and significant convection affected the coastal regions of Guangdong and Hong Kong. During the day on 8 September, under the influence of the subsistence effect associated with the outer circulation of tropical cyclone Meranti (1010) near Taiwan, the weather was very hot over southeastern China that favoured a widespread development of convective cells under this strong thermal forcing. From successive RAPIDS-NHM runs initialized in the afternoon (Fig. E-2-6a-c), intense precipitation is forecasted to develop over Guangdong coastal area and later affects Hong Kong and Pearl River Delta region. The indication on the convective development during the overnight period is consistent based on forecasts from successive model runs, though the timing on the passage of severe thunderstorm is lagged behind the actual by about 2 hours. RAPIDS-NHM also suggests the severe convective system will bring high wind gusts upon its passage. Figure E-2-7a shows the forecasted surface wind vector (white arrow) and the total wind gust (summation of forecast surface wind at 10 m level and the wind gust component depicted in color shading) at 0200 HKT 9 September, indicating that wind gusts exceeding 30 knots affect western part of the territory including the Hong Kong International Airport (HKIA). At 975 hPa, the gale force wind is forecasted near HKIA (region X; Fig. E-2-7b). From the cross section along line AB (Fig. E-2-7c), the wind speed exceeds 37 knots at 900-950 hPa levels which agrees well with an aircraft observation taken upon descend of flight towards HKIA. RAPIDS-NHM successfully forecasts the whole structure of thunderstorm and associated gust front system. Figure E-2-7c depicts the vertical cross section equivalent potential temperature (EPT in color shade) along the line AB where large EPT gradient can be seen near the gust front region (near the middle of XB). Warm moist air mass to the southwest is lifted up by the gust front while significant downdraft (Fig. E-2-7d) is found along XA that the cooler air mass is brought from about 3-4 km in altitude to near surface and spread out laterally.

With further development in data assimilation and the forecast model, the spatial-temporal error of model quantitative precipitation forecast (QPF) associated with severe convective systems could be further reduced. Moreover, through the use of an optimal phase correction technique, the model QPF can provide useful guidance on the development of significant precipitation through the blending with nowcast QPF based on extrapolation technique of radar imagery (Wong *et al.* 2009). Figures E-2-8a and b show the T+5 hour radar nowcast QPF and blending QPF at 01HKT on 9 September. It is clearly seen that RAPIDS-NHM provides signs of significant rainfall over HK during 00-01 HKT. The phase correction is applied to relocate the model QPF pattern when radar imagery is made available every 6 minutes. In this case, the blending output is also found to give a consistent scenario on the significant precipitation over Hong Kong during the overnight period. Further development will be conducted to study the techniques to improve both model forecasts and blending algorithms, in order to enhance the capability in forecasting significant convection to support both aviation and public weather services.

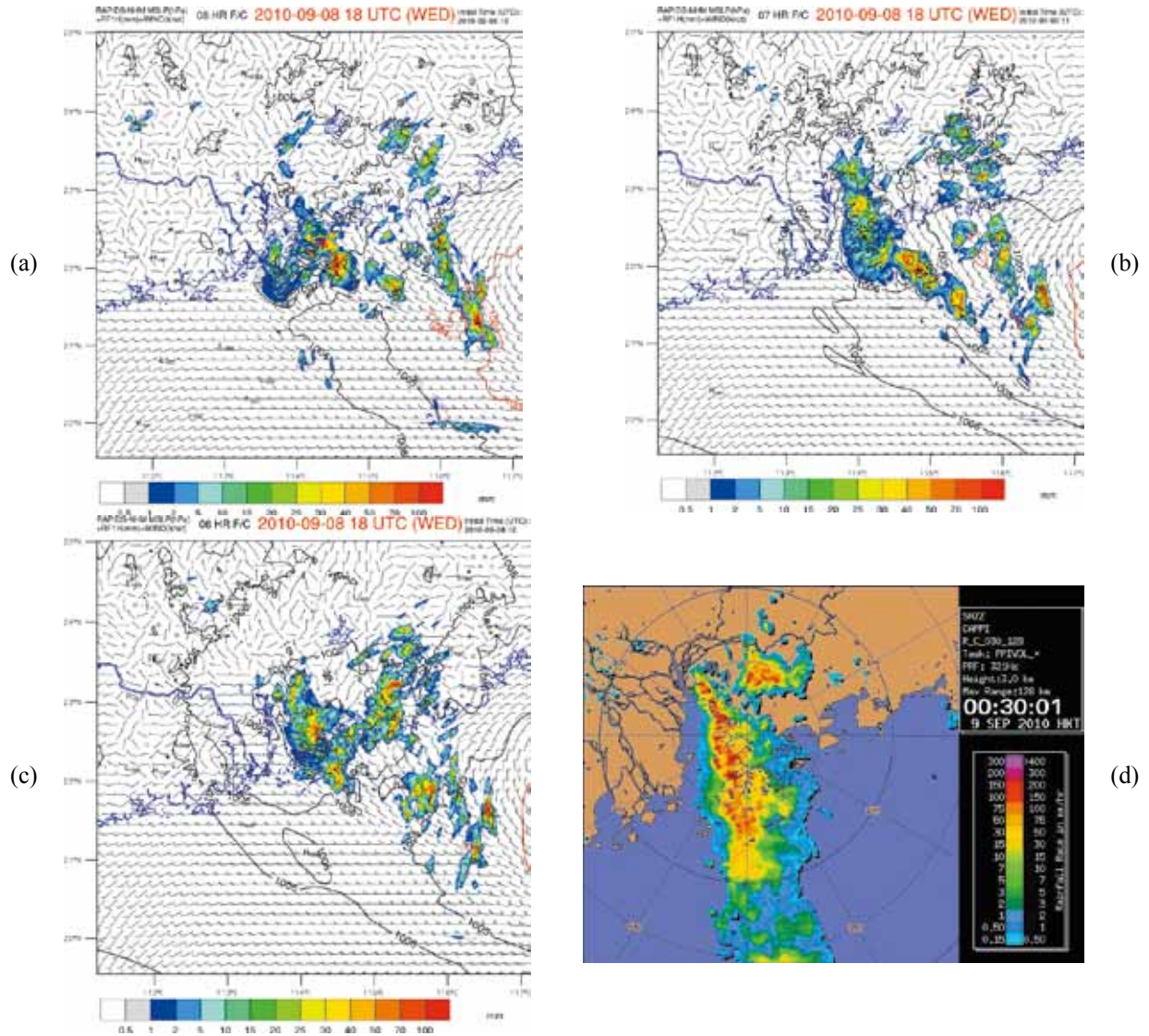


Fig. E-2-6. RAPIDS-NHM forecasts of hourly accumulated rainfall (color in mm) and mean-sea-level pressure at 02:00 HKT 9 September 2010, with model runs initialized from 10 to 12 UTC 8 September shown in (a)-(c) respectively; radar reflectivity image at 00:30 HKT 9 September 2010 shown in (d).

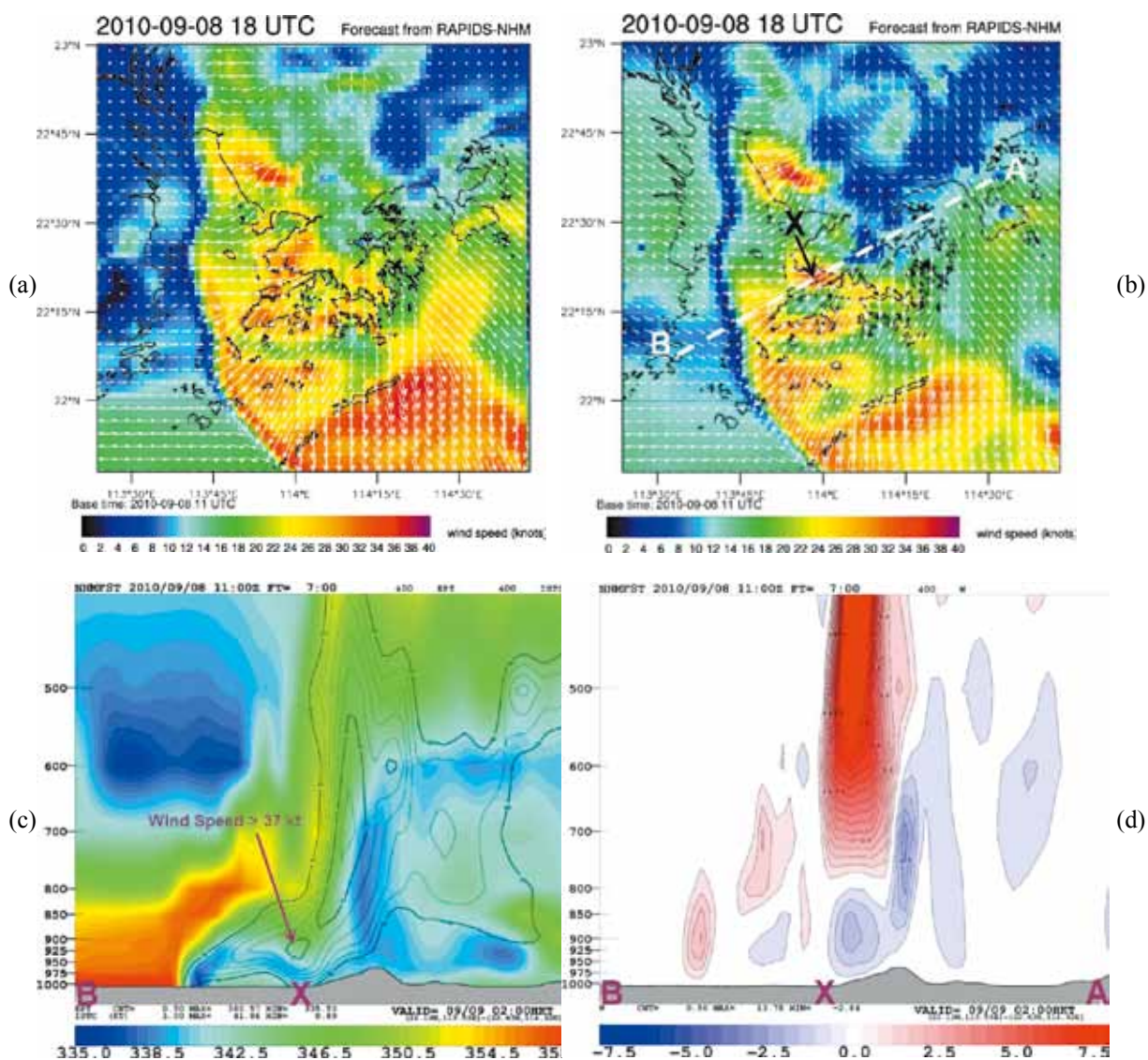


Fig. E-2-7. RAPIDS-NHM T+7h forecasts at 02 HKT 9 September 2010 on: (a) surface wind direction (white arrows) and magnitude of wind gust (color shade in knots); (b) wind speed (color in knots) and wind direction on 975 hPa; (c) vertical cross section along AB on wind speed (black contours covering areas exceeding 22 knots with an interval of 3 knots); and (d) vertical wind speed with positive value in red (in m/s) and negative in blue shading.

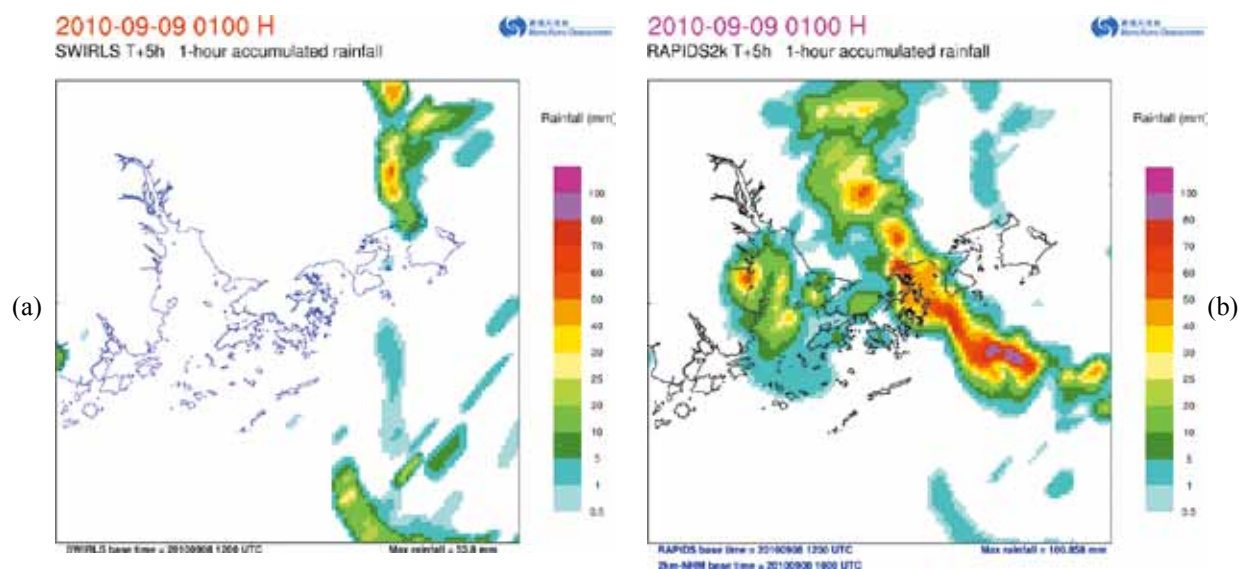


Fig. E-2-8. (a) QPF on 1-hour accumulated rainfall (color in mm) ending at 0100 HKT 9 September 2010 using radar extrapolation techniques; (b) Blending QPF by combining radar nowcast and phase corrected RAPIDS-NHM forecast.

d. Verification of NHM Analysis and Forecast

To monitor the performance of the model analysis and forecast, monthly verification is conducted for various weather elements like wind, temperature and humidity against meteorological station data. In case for Meso-NHM, 50 selected stations over the model domain are used to verify the model performance. Figures E-2-9a-d show the root-mean-square errors of Meso-NHM analysis and forecast (solid lines) for mean-sea-level pressure (MSLP), temperature, surface wind vector magnitude and relative humidity from March to December 2010. Comparing to the results from ORSM (dotted lines), the new NWP system show clear improvements owing to the use of more advanced data assimilation technique and forecast model. For instance, the RMSE of 72 hour forecast of MSLP for Meso-NHM is around 2 hPa that is smaller than that of ORSM by about 1 hPa. Improvements are clearly seen in the forecasts of surface wind and temperature that their RMSEs are generally reduced by 20-30%. Improvement in humidity forecast is also found in Meso-NHM though the gain is smaller than other weather elements. From the verification of upper level wind, Meso-NHM also shows improvements over ORSM throughout the analysis and 3-day forecast period (Fig. E2-10a-d). Using the aircraft wind data, it is also found that the performance of Meso-NHM is similar to global NWP model output that we can further enhance the development of forecast guidance and products related to upper air wind condition (e.g. en-route turbulence intensity) based on Meso-NHM output (Wong *et al.* 2011).

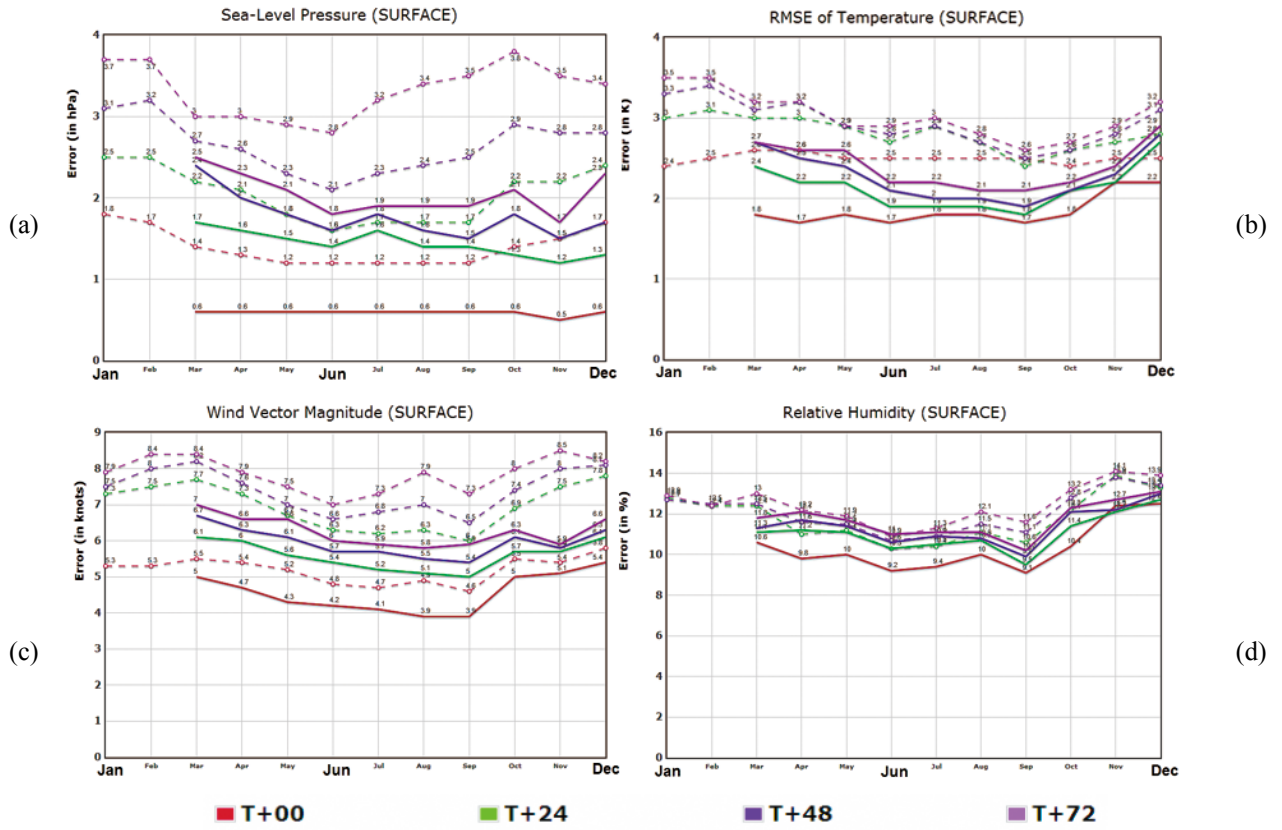


Fig. E-2-9. RMSE of analysis and forecast of surface elements from Meso-NHM (solid lines) and ORSM (dotted lines) during Mar-Dec 2010 on (a) mean-sea-level pressure, (b) temperature, (c) wind vector and (d) relative humidity.

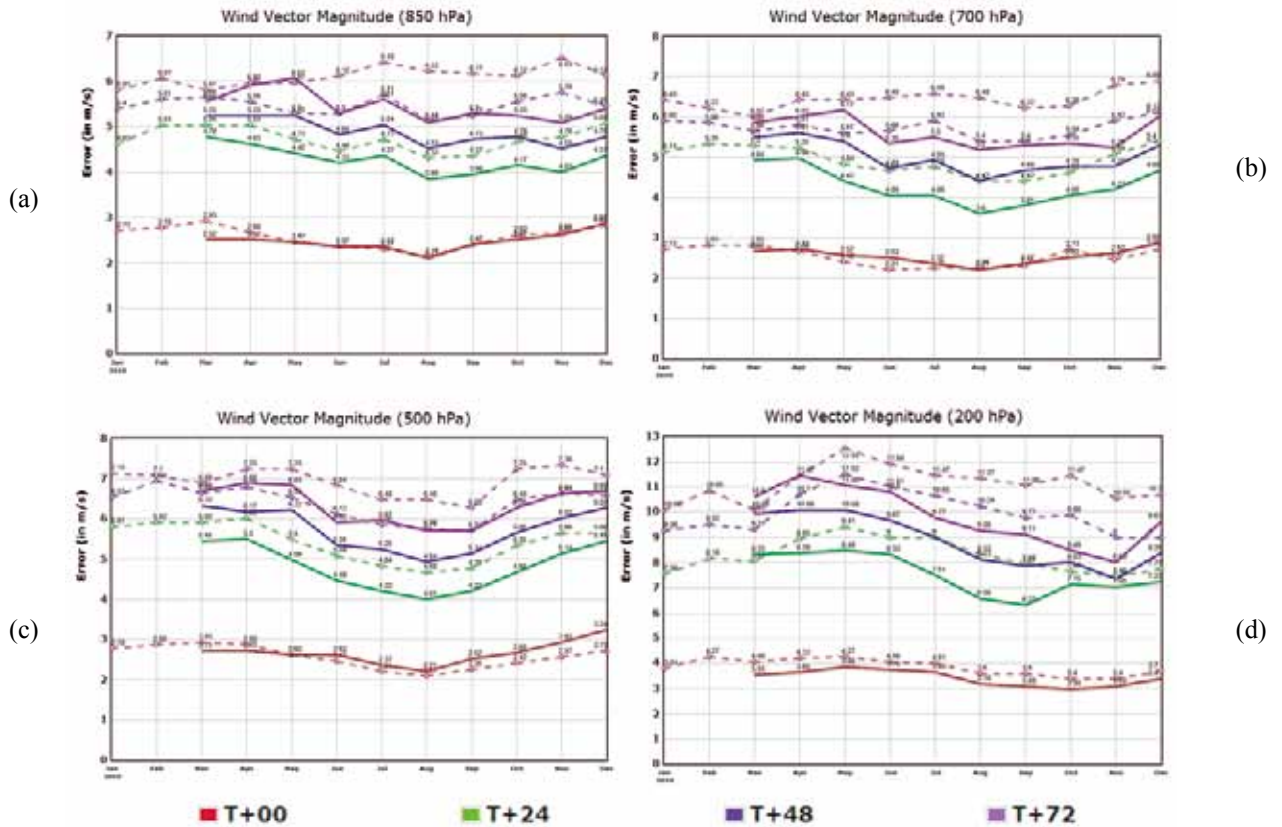


Fig. E-2-10. RMSE of analysis and forecast of wind vectors from Meso-NHM (solid lines) and ORSM (dotted lines) during Mar-Dec 2010 on (a) 850 hPa, (b) 700 hPa, (c) 500 hPa and (d) 200 hPa.

E-2-5. Summary and Future Development

The design and implementation of the AIR forecast model system - the new operational NWP model and data assimilation systems in HKO, are presented in this paper. With the increase in the model resolution, use of non-hydrostatic governing equations and more advanced model physics, the AIR forecast model system shows promising results to enhance the forecast capability of mesoscale and convective weather systems.

To further enhance the AIR forecast model system over the next few years, research and development will be made on aspects like (a) the studies of optimal parameters in physical parameterization processes, (b) development of direct assimilation of satellite microwave radiance data, (c) ingestion of radar reflectivity in JNoVA-3DVAR or retrieved moisture profiles from a separate cloud or moisture analysis algorithm (e.g., LAPS), (d) ingestion of new types of remote sensing observation (e.g., moisture and temperature retrievals from ground-based radiometer) and (e) development NHM with sub-kilometre resolution to forecast local-scale or terrain-induced severe weather phenomena in Hong Kong. Applications of NHM for aviation forecast guidance and supporting collaborative research activities on NWP will also be explored.

E-3. Available input data for NHM real-data simulation¹

E-3-1. Introduction

Until recently, NHM was able to use only JMA's original formatted data only (e.g., NuSDaS) and the available input data formats were restricted. Through the "International Research for Prevention and Mitigation of Meteorological Disasters in Southeast Asia," more datasets became available as input data for NHM and other research activities improved the usability of NHM. Previous sections of this report show some of the recent research that has been conducted using these newly available datasets.

This section briefly introduces the kinds of datasets available for NHM input and their specifications. It also lists the sections of this report where the datasets are used.

E-3-2. Available input dataset for NHM

Available input datasets for NHM are listed in Table E-3-1 with their horizontal resolutions, vertical layers, time intervals, and file formats. The data suppliers are as follows.

JRA-25 and JCDAS data are available on the JMA website (<http://jra.kishou.go.jp/>). Registration is needed to access the data for research purposes, and the data are not available for commercial purposes. In addition, JRA-55, a 55-year reanalysis dataset with a 60-km horizontal resolution and 60 vertical layers starting in 1958, is underway in JMA and will soon become available for NHM.

Global Analysis data, Meso Analysis data and two sets of ensemble forecast data (1-Week Ensemble for RSMC Tokyo region and 1-Week Ensemble forecast for Global Troposphere) are released to users outside JMA on the Meteorological Research Consortium website (<http://www.mri-jma.go.jp/Project/cons/index.html>) as part of a joint research activity between JMA and the Meteorological Society of Japan (MSJ). Foreign researchers who collaborate with a member of MSJ are eligible to access these datasets.

Forecast data by GSM and MSM of JMA are released by the Japan Meteorological Business Support Center (<http://www.jmbasc.or.jp/>). These datasets are also archived by the Research Institute for Sustainable Humanosphere at Kyoto University (<http://database.rish.kyoto-u.ac.jp/arch/glob-atmos/>) for research purposes.

Another set of high-resolution GSM forecast data for WMO Region II countries has been released by JMA and distributed to WMO affiliation member countries in region II for operational or research purposes.

NCEP-GFS forecast and analysis (including final-analysis) datasets are released by the National Climate Data Center (<http://nomads.ncdc.noaa.gov/>) with full and open access.

NHM outputs are also available for one-way self-nesting applications of NHM

¹ S. Hayashi, T. Kuroda and K. Saito

Table E-3-1. Available input datasets for NHM.

Data	Horizontal Resolution	Vertical Levels & Coordinate	Time Interval	File Format	Ensemble Members	Sections
JRA25 & JCDAS (JMA)	1.25 x 1.25 deg.	24 p-levels	Every 6 hour	GRIB1	---	C-4, C-5 D-8 (JRA55)
Global Analysis (JMA)	0.1875 deg. ~ 20km	60 η-levels	Every 6 hour	NuSDaS	---	C-3, D-1, D-2, D-3, D-4, D-5
Meso Analysis (JMA)	5km Lambert map (Japan region only)	50 z* hybrid-levels	Every 3 hour	NuSDaS	---	
GSM 1-Week EPS RSMC Tokyo region (JMA)	1.25 x 1.25 deg.	12 p-levels	Initial: 12UTC valid: every 6hour	NuSDaS	51	
GSM 1-Week EPS Global Troposphere (JMA)	1.25 x 1.25 deg.	11 p-levels	Initial: 12UTC valid: every 12hour	NuSDaS	51	D-4
GSM Forecast (JMA)	0.5 x 0.5 deg. (1.25 x 1.25 deg. before 2007- 11-21)	18 p-levels	Initial: every 6 hour valid: every 6 hour	GRIB2 (GRIB1 for 1.25deg.)	---	D-1, D-2, D-3, D-4
MSM Forecast (JMA)	0.1 x 0.125 deg. (Japan region only)	17 p-levels	Initial: every 3 hour valid: every 3hour	GRIB2	---	
GSM forecast (JMA) (only for WMO Region II)	0.5 x 0.5 deg.	22 p-levels	Initial: every 6 hour valid: every 3hour	GRIB2	---	
GFS Forecast (NCEP)	1.0 x 1.0 deg. 0.5 x 0.5 deg.	27 p-levels	Initial: every 6 hour valid: every 3 hour	GRIB1 GRIB2 for 0.5 deg.	---	C-1, C-2 C-8
GFS (Final) Analysis (NCEP)	1.0 x 1.0 deg. 0.5 x 0.5 deg.	27 p-levels	Every 6 hours	GRIB1 GRIB2 for 0.5 deg.	---	C-7
NHM outputs (JMA)	any	any	any	NuSDaS	---	